

# Chapter 17

## Application of Lasers to Microwave Standards

The advent of the laser changed the whole character of atomic frequency/time standards in a number of fundamental respects: from the manipulation of the internal quantum states of the reference particles, to cooling of the center-of-mass motion and prolonged observation of single isolated reference particles. The former application introduced a radical change in the way the cesium clock transition is observed, and the latter made possible, in one revolutionary advance, the realization of the ideal goal that motivated the original pre-laser forays into field suspension of ions, embodied in the  $\text{Hg}^+$  ion microwave resonance experiment at NASA. That goal was to completely isolate the reference particle from its environment, and to observe its true resonance, free from Doppler shifts and any uncontrolled random perturbations. In this chapter we will touch on the application of lasers to atomic frequency standards in the microwave region of the spectrum, and take up their role as frequency standards in the optical region in later chapters.

### 17.1 Observation of Individual Ions

#### 17.1.1 Introduction

One of the most significant developments made possible by the laser revolution is the direct optical observation of *individual* atomic ions. We can, by focusing a resonant laser beam onto the region of confinement of the ions, actually scatter enough photons to literally see the discrete particle nature of whatever is doing the scattering. It is true that even in the very early days of the Paul trap, the sensitivity of ion detection by electronic means was pushed to the point of resolving the discreteness of ions in a cloud, but now with the laser, the signal-to-noise ratio is incomparably higher, and *single* ions are observed for extended periods of time.

This remarkable feat of directly observing individual cold ions as spots of light “crystallized” in a Paul trap was, of course, the culmination of the work of many

pursuing the many aspects of the interaction of radiation with matter, which the special properties of lasers made possible. In the beginning, estimates suggested that the enormous signal-to-noise advantages of using resonance scattering of laser radiation held out the hope that the observation of individual atomic particles was within reach. Knowledge of how close one is to resolving individual particles starts with a theoretical estimate of the number of ions implied by the observed intensity of the scattering, based on what is known about the ion cross section for this process. This is useful in assessing progress toward the ultimate goal; however, the approach to resolving individual ions is signaled by the appearance of stepwise variation in the scattered intensity, jumping between a finite number of discrete levels, when ions are created or removed from the trap.

The ions are usually created by random ionizing collisions between electrons and the parent atoms, and a statistically fluctuating number of ions are accumulated in the trap during any given filling period. However, the frequency of occurrence, that is, the probability of different values of that number, follows a determinate law. If, as is generally the case, the number of available parent atoms is infinitely large compared to the number actually ionized, we can assume that any given ion had an equal probability of becoming part of the ion population at any time during the filling period. In that case it can be shown that the frequency of a given ion number follows what is called the *Poisson distribution*. If we represent the *average* number of ions trapped by  $\langle n \rangle$ , then the probability  $p(n)$  that precisely  $n$  ions are trapped is given by the following:

$$p(n) = \frac{\langle n \rangle^n}{n!} e^{-\langle n \rangle}. \quad 17.1$$

Figure 17.1 shows a plot of the Poisson distribution, giving the relative probability of a cluster being formed with different total numbers of ions, for a given average number of ions trapped. When this number is extremely large, as in the original

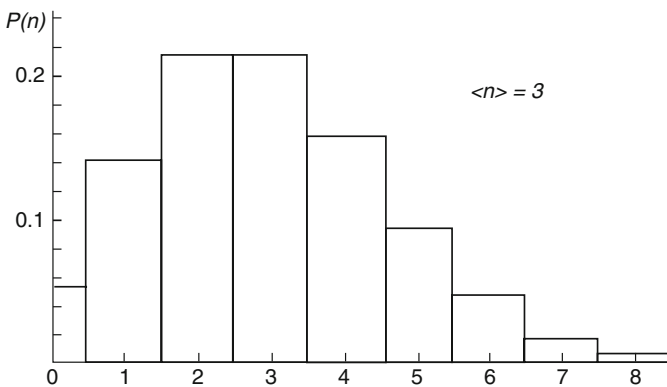


Figure 17.1 The Poisson distribution in the number of stored ions

$\text{Hg}^+$  ion experiment, the discreteness in the fluorescent signal measuring the ion number would manifest itself only as a small fluctuation, namely *shot* noise. It is only when the signal from only a few ions is observed with a large signal-to-noise ratio that individual ions are clearly discernible.

Through the ability to resolve individual ions in the trap it becomes possible to limit the ion population to a single ion, or at most a string of individual ions, located at points where the amplitude of the Paul high frequency field is zero; that is, where the micromotion, whose energy is determined by the field amplitude, is zero. In the classical Paul trap there is only one point where the field amplitude is zero, namely at the center of the trap. Clearly then, if signal-to-noise limitations required many contributing ions to be observable, their mutual repulsion would prevent their all occupying the center, and the micromotion of those repelled from the center would set a lower limit to the energy, since the laser cooling affects only the secular motion, not the micromotion. It follows that for a cloud of ions, interaction between ions may not only perturb their internal quantum states, but will also limit how far the temperature can be lowered, and the (second-order) Doppler effect thereby eliminated.

As explained in an earlier chapter, collisions involving an ion in the high-frequency electric field of a Paul trap result in abrupt changes in ion energy due to a change in the phase of its secular motion. Now the ability to observe an isolated single ion means that ion-ion collisions can be eliminated; all that would remain is the possibility of collisions with background gas particles in the vacuum system. This means that now the experimental burden is on the ultrahigh vacuum system to maintain a sufficiently low particle density in the ion trap. In the case of an element such as mercury with its high vapor pressure, an effective approach is to use *cryogenic pumping*, that is, lower the temperature of the system to the point where everything (except helium) freezes! This is accomplished by immersing the system in liquid helium. A less drastic approach is to rely on one of the triumphs of modern vacuum technology, the titanium ion pump, which makes it possible to reach pressures as low as  $10^{-10}$  Pa, if extreme care is taken in the design and construction of the system. Although this is far from a “perfect” vacuum (by comparison, interplanetary space has an average particle density more than 10,000 times smaller), nevertheless, the particle density is so low that the average time between collisions involving the ion and a background particle can be several days! Thus although a collision may result in some increase in energy, so much time elapses between collisions that the average rate of energy increase is extremely small. To really benefit from this low average collision rate, the trap must obviously be designed so that *several* collisions are required before the ion acquires sufficient energy to escape.

### 17.1.2 Trap operating conditions

The design of the physical setup for laser cooling of ions in a Paul trap must begin with the design of the trap itself. A particularly important physical parameter at

our disposal is the *secular* oscillation frequency of the ion. This, it will be recalled, is given by  $\beta\Omega/2$ , where  $\beta$  is approximately given by  $\beta^2 \approx a + q^2/2$  under the so-called *adiabatic* condition, where an ion oscillates at the field frequency with a small amplitude (the micro-motion) as it executes its slower oscillation about the trap center (the secular motion). In this case the ion oscillation spectrum is dominated by the frequency  $\beta\Omega/2$  with components at the frequencies  $(2 + \beta)\Omega/2$  and  $(2 - \beta)\Omega/2$ , which are very much weaker. There are two other important parameters: the inherent *optical* resonance line width of the ion and the spectral line width of the laser light. It simplifies the description of the Doppler cooling process considerably and can render it effective in reaching the ultimate zero point energy in the trap if the laser line width is smaller than the optical resonance line width of the ion, and if in turn, the latter is smaller than the frequency separation of the Doppler sidebands, so that they are well resolved.

Since optical transitions suitable for laser cooling must occur with the ions presenting a relatively large cross section to the beam, their spectral line widths (due to the high transition probability) should not typically be far below the megahertz range; this implies that the ion oscillation frequency  $\beta\Omega/2$  should be at least on the order of megahertz, and thus for  $\beta \approx 0.1$  (say) the field frequency  $\Omega$  must be in the tens of megahertz range. Based on these considerations we can now arrive at the specifics of a typical trap design suitable for laser cooling of ions. For example, if we assume a field frequency of  $\Omega/2\pi = 10$  MHz, then for the  $\text{Hg}^+$  ion we find  $q_r = 2.4 \times 10^{-10} V_0/r_0^2$ . We are at liberty to choose the exact value of  $q_r$ , provided that it falls within the stable region of the  $a$ - $q$  diagram; if we choose  $q_r = 0.05$  and  $r_r = 1$  mm, then the required radio-frequency amplitude would be  $V_0 = 210$  volts. We note that the assumption of a relatively high oscillation frequency for such a massive ion has led us to trap dimensions on a miniature scale compared with those used in the pre-laser mercury ion standard. The difficulty of attaining precision and mechanical stability in the construction of such miniature traps has elicited a variety of ingenious electrode geometries; the only essential requirement is that a saddle point be produced in the electric potential to trap an ion.

The maximum kinetic energy an ion may have while confined in such a trap can be readily computed if we recall that under the assumed conditions, the average kinetic energy of the high-frequency oscillation at frequency  $\Omega$  is equivalent to an electrostatic potential that simply adds to the applied static potential in determining the slow oscillation at frequency  $\beta\Omega/2$ . Using the formula  $\beta^2 \approx a + q^2/2$ , we can show that the maximum energy is  $E_{\max} = (eU_0/2 + eqV_0/8)$ . In the example we have chosen, this has the numerical value on the order of 1.25 electron volts, which, to give an idea of relative magnitudes, is the mean energy of a particle at a temperature of about 14,500°K.

The initial filling of the trap with ions is achieved through ionizing collisions between electrons in a beam intersecting a beam of parent atoms in the trapping region. Once the trap is filled, a process that takes only a fraction of a second, the beams must be interrupted in order on the one hand to minimize the density of background particles and on the other to remove any distortion of the electric

field the charged electrons may produce. Since the intention is to trap only a few, and ultimately only one super-cooled ion, the large initial ion population having an energy spread reaching perhaps a maximum of 1.25 electron-volts must be reduced to only those having a small fraction of that energy. This can be done, of course, by lowering the amplitude of the high-frequency field for a short time, thereby reducing the maximum energy and allowing the more energetic ions to escape.

## 17.2 Optical Detection of Hyperfine Transitions

### 17.2.1 Laser System Design Considerations

The design of the laser system is determined primarily by the wavelength of the resonance fluorescence transition in the particular atomic species under study. Experimental work has been published on a number of ions in addition to the  $\text{Hg}^+$  ion; for example, the alkali-like ions of the heavy alkaline earth elements, principally strontium  $\text{Sr}^+$ , and barium  $\text{Ba}^+$ , as well as the ytterbium ion  $\text{Yb}^+$ . From the point of view of constructing a suitable laser system, the  $\text{Ba}^+$  ion with a resonance fluorescence wavelength in the green region of the spectrum at a wavelength of  $\lambda = 493.4 \text{ nm}$ , is the least demanding. Unlike the other ions, whose resonance occurs in the ultraviolet region of the spectrum, the  $\text{Ba}^+$  ion resonance wavelength falls in a range for which there exists an adequate dye (coumarin 102) to use in a tunable dye laser to generate the desired wavelength directly.

Once we have successfully synthesized the desired optical frequency with sufficient spectral purity for laser cooling the ion, we have in effect solved another problem we faced in constructing a microwave standard, namely pumping the ions preferentially into one of the hyperfine levels. This, it will be recalled, was first accomplished in the mercury ion resonance experiment—and is still used in a number of portable embodiments of the  $\text{Hg}^+$  ion microwave standard—by using the fortuitous overlap of the ion resonance line from a mass 202 mercury lamp with just one of the hyperfine components in mass 199 ion fluorescence spectrum. With a resonant laser source tuned to that same wavelength and having a spectral width as small as 1 MHz, the pumping problem is solved. In fact, if the intent is only to cool the ions, the hyperfine pumping that will inevitably occur is a problem that must be circumvented, since the ions tend to end up in the non-absorbing hyperfine sublevel of the ground state.

### 17.2.2 “Electron Shelving” Method of Resonance Detection

The extraordinary degree of isolation that a single trapped ion enjoys means that for very long-lived upper quantum states, an extended interaction time is possible with a probing field, allowing extremely narrow resonant transitions to the

ground state to be observed. These long lived states include the familiar magnetic hyperfine states, as well as *metastable states* from which optical transitions are “forbidden” (for electric dipole), and only electric quadrupole or higher order electric octupole transitions are “allowed”. In the  $\text{Hg}^+$  ion case, sharp resonant transitions are present involving both the microwave hyperfine states and optical metastable states with unprecedented Q-factor; in the latter case in excess of  $10^{12}$ ! Unfortunately, the very fact of the resonance transition having a small spontaneous emission probability also means that it will have a small absorption cross section, making it unsuitable for observing the resonance *directly* through the resonantly scattered photons. Simply increasing the intensity of the resonance detection field to the point of enhancing the transition rate is ruled out since it will *power broaden* the resonance frequency, compromising the essential objective of an ultra-narrow resonance.

As we saw in the case of the Cs and Rb standards, the resonance must be observed by an indirect “trigger” method, in which the rather weak exchange of energy involved in the microwave reference transitions causes a much larger observable effect: in the Cs standard it changed the trajectory of the cesium atoms, and in the Rb and  $\text{Hg}^+$  ion standards the absorption of resonant microwave photons affected the number of very much more energetic optical pumping photons to be absorbed in “allowed” transitions between one of the reference magnetic substates and other states.

In the context of a single ion stored free of perturbations for days, it is possible to manipulate its quantum states and separate in time the functions of inducing transitions on the one hand and detecting whether they occurred on the other. This is achievable if the resonance is monitored using a strong fluorescence transition linking *one* of the reference states, but with a wavelength far removed from that of the reference transition. The monitoring beam can then simply be *turned off* while the reference transitions are being induced by a weak probing field, and then turned back on to establish whether transitions were indeed induced.

Prior to the advent of single ion spectroscopy, a precursor to this approach would have been described as a *double resonance* method, in which the relative intensity of the fluorescence at one resonant wave length is monitored as the other is swept through a second resonance involving a common level. With a single ion controlling the fluorescence, the method takes on a stark, on-off aspect. The ion is either in the lower reference state or the upper state. If the reference states share a common lower state with the states between which a strong fluorescence is allowed, then the full intensity of that fluorescence will either be present or totally absent depending on which of the two reference states the ion occupies! As long as the ion remains in the upper reference state there will be zero fluorescence; not until it is induced to make a transition (or spontaneously decays) down to the lower state does the fluorescence again appear in all its glory. This process has been dubbed using a brilliant metaphor: *electron shelving*, a term attributed to H. Dehmelt.

### 17.2.3 The Signal-to-Noise Ratio

While the suspension of an individual cold ion provides an ideal reference, free from perturbations and Doppler shifts, the signal-to-noise ratio in determining the precise center of its resonant frequency will, in addition to photon shot noise and possible fluctuations in the laser beam frequency and intensity, be limited fundamentally by what has been called *quantum projection noise*. This simply reflects the statistical nature of the occurrence of a discrete quantum transition. It is analogous to the *shot noise* described in Chapter 4. The roles of the different types of noise sources in the present case in which the number of ions is small, are reverse of what it had been in the original ion cloud standard, with its weak fluorescent intensity. There the effect of quantum transition noise on the signal-to-noise ratio was negligible compared with the shot noise of the fluorescent photons because the number of ions undergoing transitions is much larger than the number of photons detected. In contrast, here the resonant laser scattering from a cluster of ions is so large that in practice the photon shot noise may well be less important than frequency and intensity instabilities in the laser source. Ultimately, however for scattering by a single ion of a large number of photons from a stable laser, the fundamental quantum noise is expected to dominate.

To bring out quantitatively the fundamental limits to the signal-to-noise ratio, we will consider the bare essentials of a scheme to observe the microwave clock transition in  $^{199}\text{Hg}^+$  ions. In what follows we will often speak of ions, in the plural, when in fact only one ion may be involved; it is assumed that an ensemble average taken over many ions is the same as an average taken over many identical repetitions of the same measurement on one ion.

Assume then that we use one laser to both optically pump the hyperfine states and to detect the microwave clock transition between them; a straight forward extrapolation of the method first used by the author on a mercury cloud. Since the clock transition must be observed “in the dark” to avoid light shifts in the frequency, we assume the following sequence of events: 1. The laser is turned on to pump the ion out of the absorbing lower hyperfine state into the other non-absorbing state, at which point the fluorescence tends to zero. 2. The laser beam is cut and the microwave field applied to induce the clock transition, thereby coherently mixing the two sublevels; assume this continues only until the ion has a probability of  $1/2$  of having made a transition. This essentially quantum mechanical description of the ion being in a “mixed state” is counter-intuitive of course and is the basis of the so-called “Schrodinger’s cat” paradox, in which the cat doesn’t know if it’s alive or dead! 3. The laser beam is again turned on and if the ion has made the clock transition, the fluorescent photons radiated by it are counted. Suppose that the *average* photon count *per ion* (if there are more than one) taken over many repetitions of the identical procedure is represented by  $\langle N_p \rangle$ , then the rms deviation of the individual photon counts from the mean is given by  $\sqrt{\langle N_p \rangle}$  (see Chapter 3). We should note that the photon count so obtained does not give directly a measure of the probability of the ion having made the transition, since it is being

pumped into the other state in the act of counting the photons. Ideally we should have another laser exciting a *cycling* optical transition for a direct and efficient way of detecting the probability of an ion being in a particular state. If we assume we have a cluster of  $N_i$  ions in the trap contributing to the total photon count, then there will also be a statistical fluctuation in the actual number of ions that have made the clock transition and are contributing to the fluorescent photon count. As we saw in Chapter 3 in discussing the random walk problem, the rms deviation is given by  $\langle \Delta N_i^2 \rangle = N_i p(1 - p)$ , where  $p = 1/2$  according to our assumption.

We are now ready to compute the total fluctuation in the photon number detected arising both from the photon shot noise for each ion and the fluctuation in the number of ions that actually underwent the clock transition. Since these numbers are independent they are quadratically combined, that is,

$$\langle \Delta N_d^2 \rangle = \frac{1}{2} \langle N_p \rangle N_i + \frac{1}{4} \langle N_p \rangle^2 N_i \quad 17.2$$

For  $\langle N_p \rangle \gg 1$  the rms fluctuation  $\sigma_p$  is given by:

$$\sigma_d \approx \frac{1}{2} N_p \sqrt{N_i} \quad 17.3$$

#### 17.2.4 The Dick Effect

In both the confined ion resonance standards and the cesium standards, whether of linear or fountain geometry we have passive devices which require a local oscillator to “interrogate” and lock on to the frequency of the reference ion or atom. In both cases the interrogation must of necessity be interrupted during part of each cycle of measurement during which the local oscillator receives no corrective feedback signal in the servo loop. This periodic pulsed interaction of the reference particles with the probing field has been shown first by J. Dick in 1989, in the context of a mercury ion standard, to cause noise in the local oscillator to degrade the long term stability of the standard (C. Audoin, 1998). The effect is noticeable in recent ion and fountain standards where interruption times are of relatively long duration, when the local oscillator is free to run.

Since the control on the local oscillator is discretely periodic it is expected that an analysis of the system would involve *sampling theory*, a discipline that is of course at the core of analog-to-digital conversion technology. An important concept in this field is *aliasing*, in which a rapidly varying function is sampled at too low a frequency resulting in “aliases” at lower frequencies that do not represent the given function. In sampling a function the applicable criterion to avoid aliasing is a theorem due to C. E Shannon, called the *Sampling Theorem*, which states in effect that in order to represent a given function  $f(t)$  exactly, it is necessary to sample the function at a frequency greater than twice the highest frequency component in the function.



In the Dick effect the high frequency noise of the local oscillator is aliased by the slow sampling rate to frequencies close to the signal, resulting in spurious frequency shifts in the standard.

### 17.2.5 Ramsey Time-Separated Excitation

In order to interrogate the ion, that is, determine what frequency of the field resonates with the reference transition, a version of the Ramsey separated fields method is adopted. We recall that in the cesium standard the resonance is observed by making the cesium atoms pass through two spatially separated phase-coherent microwave field regions, produced in the *Ramsey cavity*. As Ramsey originally pointed out, the method can be applied equally using phase-coherent fields separated in *time* rather than space; this is not surprising, since transitions obviously have to do with the evolution of quantum states in time. The ions are subjected to two *coherent* microwave bursts of precisely controlled intensity and duration, separated by a precise time interval. (Coherent here simply means that it is as though the two bursts are parts of the same continuous wave). The Ramsey technique is important in realizing experimentally the sharpness of resonance implied by the long radiative lifetime of a suspended ion by suppressing the effect of residual fluctuations.

In discussing transitions in the Ramsey field in the cesium standard, for the purposes of providing a concrete picture of the process, we spoke in terms of the motion of a magnetic dipole in a magnetic resonance experiment, in which a transition can be visualized as a rotation of the dipole axis with respect to a static magnetic field direction. The same analogy applies here. In quantum terms, the effect on an ion of a field inducing hyperfine transitions is to put it in a nonstationary quantum “mixed” state involving both initial and final states, with a magnetic moment varying periodically at the transition frequency. The time development of the transition is characterized by the *Rabi nutation frequency*  $\omega_R$ , which is proportional to the amplitude of the field inducing the transition. Now, we recall that in quantum mechanics the absorption and stimulated emission of radiation are treated on an equal footing, and that if an otherwise free ion is kept in the microwave field, it will keep going back and forth between the two hyperfine states. An ion acted on by a resonant field characterized by the Rabi frequency for a period  $\tau$  will, starting in one state, make a complete transition to the other state when  $\tau$  reaches the value given by  $\omega_R \tau = \pi$  and will return to the original state if it continues until  $\omega_R \tau = 2\pi$ . In general, it can be shown that the probability that an ion starting in one state will after some time  $t$  have made a transition to the other state is given by the following:

$$P = \frac{\omega_R^2}{(\omega - \omega_0)^2 + \omega_R^2} \sin^2 \frac{1}{2} \sqrt{(\omega - \omega_0)^2 + \omega_R^2} t \quad 17.4$$

where  $\omega$  and  $\omega_0$  are the (angular) frequencies of the field and ion transitions respectively. We easily verify that at resonance, when  $(\omega - \omega_0) = 0$ , the probability that a transition has occurred,  $P$ , has the value one when  $\omega_R \tau = \pi$ , as stated above. The result is a good deal more complex when there are two separate periods during which the ion is subjected to the resonant field. A classic account of the quantum theory of spectral line shape with this arrangement was given by Norman Ramsey back in the early 1950's. Our only interest is in the line shape in the neighborhood of the central maximum. For values of the frequency such that  $(\omega_0 - \omega) \ll \omega_R$  Ramsey's result takes the following form:

$$P(\tau) \approx \frac{1}{2} \sin^2(\omega_R \tau) [1 + \cos(\omega - \omega_0)T] \quad 17.5$$

From this we see that  $P(\tau) = P_{max}/2$  when  $(\omega - \omega_0) = \pm\pi/(2T)$ ; hence the full width (in Hz) at half the maximum is  $1/(2T)$ , where  $T$  is the time interval between the two Ramsey interaction periods.

In the usual design, the amplitude of the field (and therefore the Rabi frequency  $\omega_R$ ) and duration  $\tau$  of each of the two time-separated bursts are chosen such that  $\omega_R \tau = \pi/2$ . Now, if the field frequency is tuned to exact resonance with the ion transition frequency, then during the free time the ion spends between burst, the oscillating moment of the ion remains exactly in phase with the field, so that when the second burst begins, the situation is indistinguishable from the end of the first burst. In this case, at the end of the second burst  $\omega_R \tau = \pi$ , and the ion has completed its transition to the other state. The important point to make here is that if during the relatively long interval between bursts the ion transition frequency varies slightly, but randomly, the phase of the ion moment at the end of that interval tends to average out such frequency fluctuations. If the field is mistuned so that  $(\omega - \omega_0)$  is not zero, then a phase difference  $\Delta\phi = (\omega - \omega_0)T$  will develop between the ion moment and the field during the period  $T$  between bursts, and the probability of a transition by the end of the second burst will be less. Since only the *relative* phase between the ion moment and the field at the end of the free period  $T$  is physically significant, it follows that a mistuning leading to a phase difference of  $\Delta\phi$  is indistinguishable from one giving a phase difference of  $\Delta\phi + 2n\pi$ , where  $n$  is a whole number. Figure 17.2 illustrates the periodic nature of the transition probability as indicated by the scattered photon counts plotted against the frequency mistuning of the field.

We are now ready to estimate the expected stability of a standard locked to the resonance observed in this way. Following what has become standard practice in a digital servo design, the interrogating field frequency is stepped symmetrically about the maximum between the two half-intensity points in the fluorescent output; that is between  $(\omega - \omega_0) = +\pi/(2T)$  and  $(\omega - \omega_0) - \pi/(2T)$ . We must calculate the fluctuation in *frequency* of the standard caused by the fluctuation in the photon count described above; this requires knowledge of the rate at which

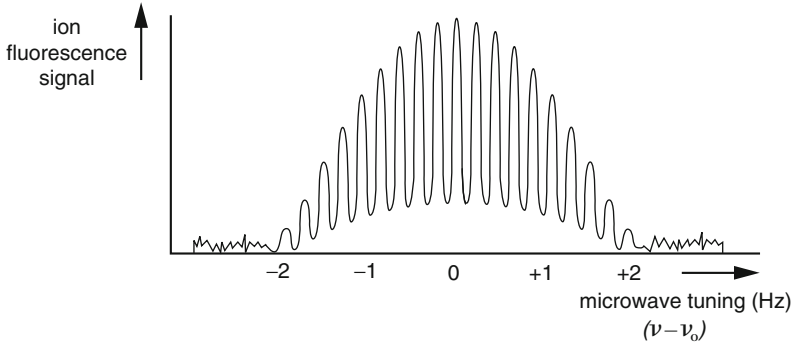


Figure 17.2 The periodic resonance signal seen in a time-separated Ramsey field

the photon count varies with the frequency at the sampling points. This is simply given by :

$$\left[ \frac{dN_d}{d\omega} \right]_{(\omega - \omega_0) = \pi/2T} = \frac{N_p N_i T}{2} \tag{17.6}$$

where as before the number of photons counted per ion in the fluorescing state is  $N_p$ , and  $N_i$  is the number of ions. It follows that the fractional frequency fluctuation statistically averaged over a total measuring period which is conventionally represented by the symbol  $\tau$ , (not to be confused with the duration of the Ramsey microwave bursts), that is over  $\tau/(2T)$  independent detection cycles, is given by:

$$\sigma_\omega = \frac{1}{\omega_0 \sqrt{N_i T}} \tau^{-1/2} \tag{17.7}$$

### 17.3 The NIST Mercury Ion Microwave Standard

While the pre-laser  $\text{Hg}^+$  ion standard achieves high performance in a compact portable unit, the use of laser cooling takes it to an altogether new level of sophistication and accuracy; but with present technology it is no longer portable. This is not, of course, a consideration for a *laboratory standard*, and as such its accuracy can be enhanced by laser cooling not only by the near elimination of the second-order Doppler effect, but also by reaching new limits on the other factors known to affect the hyperfine frequency, that is, ambient electric and magnetic fields. Thus the act of cooling the ions reduces their motion to where the high frequency field amplitude approaches zero; hence the already minor effect the electric field has on the magnetic hyperfine splitting becomes entirely negligible.

Interest in the use of  $\text{Hg}^+$  as the basis of both a microwave and optical frequency standard has mainly been implemented by Wineland and his group at the Time and Frequency Division of the (U.S.) National Institute of Standards and

Technology (NIST). For the microwave standard at 40.5 GHz, a linear form of the Paul trap, illustrated schematically in Figure 12.8, was built to enable several ions to be crystallized along the axis where the high frequency field is zero. The absence of the ion micro-motion there prevents the ions from gaining kinetic energy through collisions, thereby allowing the cooling laser to be turned off during the interrogation period.

The optical transitions involved in the operation of the standard involve the quantum states already introduced in Chapter 13, and reproduced here in Figure 17.3. The ions are Doppler cooled using a laser beam tuned below the frequency of the transition between the states  $^2S_{1/2}, F = 1$  and  $^2P_{1/2}, F = 0$ . During the Doppler cooling phase it is necessary that the ions not be pumped into a “dark” (non-absorbing) state. Ideally, if the laser radiation driving the cooling transition were spectrally pure the ion population would cycle between just the two named states ( $F = 0 \rightarrow F = 0$  is forbidden). In practice some excitation of the neighboring upper state  $^2P_{1/2}$  is caused by a wing of the laser spectrum leading to transitions into the lower  $^2S_{1/2}, F = 0$  state. This necessitates the application of another laser beam during the Doppler cooling phase, to drive the transition  $^2S_{1/2}, F = 0$  to  $^2P_{1/2}, F = 1$ . Of course during the hyperfine state pumping phase, this would be blocked allowing the ions to accumulate in the  $F = 0$  sublevel of the ground state. At this point in the sequence of operations the laser beams are interrupted and the microwave interrogating field applied in the form of Ramsey bursts separated by longer intervals  $T$ . Finally the transition  $^2S_{1/2}, F = 1 \rightarrow ^2P_{1/2}, F = 0$  is excited to determine the number of ions that have made a microwave transition by counting the fluorescent photons.

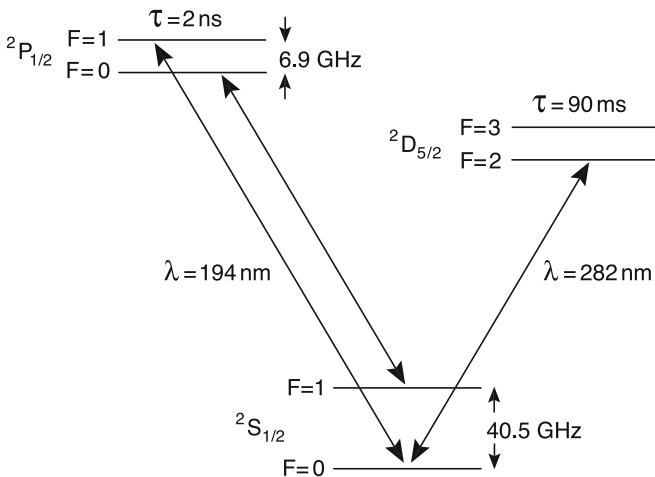


Figure 17.3 The relevant quantum energy levels of  $^{199}\text{Hg}^+$  ion

The design of the laser system to generate the ultraviolet wavelength at 194 nm, required for cooling and hyperfine pumping the  $^{199}\text{Hg}^+$  ion, presents a challenging problem of optical frequency synthesis. This wavelength is impossible to produce directly since it is well beyond the range of dye lasers, and even to produce it as a second harmonic in a crystal, starting with a laser having twice the wavelength, is ruled out because of the difficulty of finding a crystal to meet the phase matching requirement, as discussed in Chapter 14. Radiation absorption at this ultraviolet wavelength severely limits the choice of suitable crystals.

In the work described by the NIST group at Boulder, non-linear crystals of potassium pentaborate designated KB5, and beta barium borate, BBO, are used to generate the *sum-frequency* of a fundamental beam at  $\lambda = 792$  nm and one at  $\lambda = 257$  nm, yielding a beam at the desired 194.03 nm. The  $\lambda = 257$  beam is obtained by frequency doubling the  $\lambda = 515$  nm output of an argon ion laser forced to operate at a single frequency by a temperature tuned étalon. The non-linear frequency doubling is achieved using a BBO crystal with a face cut at the Brewster angle to the axis, placed at the beam waist in a ring cavity tuned to resonance with and mode matched to the input  $\lambda = 515$  nm beam, and serving to greatly enhance the intensity of the optical field at the crystal, thereby increasing the non-linear conversion to the second harmonic  $\lambda = 257$  nm. Provision is made to finely tilt the angle of the crystal to meet the phase matching condition.

The other laser beam at wavelength  $\lambda = 792$  nm is derived from a master diode laser with an external cavity that is stabilized ultimately with reference to an iodine-stabilized argon ion laser. This is followed by a mode-matched tapered amplifier acting as a “slave” laser, phase-locked to the former.

Two resonant overlapping ring cavities have the intracavity beams coincide at the common waist where the Brewster-cut, sum-frequency BBO crystal is mounted. Both fundamental beams propagate as ordinary rays through the crystal, while the sum-frequency beam at  $\lambda = 194$  nm propagates as an extraordinary ray. The incidence angles of the fundamental beams into the ring cavities must be finely adjusted to ensure that they are collinear inside the crystal. In this way it is reported by Berkeland, et al. (Berkeland, 1998) that as much as 2m W of radiation at the  $^{199}\text{Hg}^+$  pumping wavelength was generated.

The extraordinary sharpness of the resonance made possible by laser cooling has meant that the more common methods of achieving ultrahigh vacuum and magnetic shielding are no longer adequate. The group at NIST have proposed (Poitzsch, 1994) that both concerns can be effectively met by operating the linear ion trap system at the temperature of liquid helium (around 4.2°K). Since all forms of matter (except of course helium itself) are frozen at this temperature, with vapor pressure so small that it would be a challenge to measure it, this is the ultimate method of reducing background pressure. It of course introduces a whole new level of complexity into the picture, involving the technology of cryogenics. The ion trap system must be immersed in a liquid helium bath in a *cryostat*, consisting of two Dewars (thermal isolation chambers): an inner one containing the liquid helium, and an outer one filled with liquid nitrogen. Since the liquid helium has to be continuously

replenished, a constant source is obviously required. Apart from residual helium in the ion trap vacuum system, whose pressure can be maintained well below  $10^{-7}$  Pa with ion pumps, cryogenic pumping then would put an end to the vacuum problem.

Furthermore, such a cryostat would also enable the ultimate in magnetic shielding: a superconducting metal enclosure. A superconductor is a material that, below a certain critical temperature  $T_c$ , conducts electricity with zero resistance. The phenomenon was first observed in mercury at the temperature of liquid helium and has since been found to occur in many elements and a large number of alloys and compounds, including the high- $T_c$  oxides discovered in 1985. The most common alloys are those of niobium with titanium or tin ( $Nb_3Sn$ ), which has  $T_c = 18^\circ\text{K}$ . However, a superconductor is not just a body with zero electrical resistance; it was shown by Meissner in 1933 that if a material is placed in a magnetic field and then cooled below its transition temperature, it assumes a unique state in which the magnetic field is “expelled” from its interior, a phenomenon known as the *Meissner effect*. This effect, plus the fact that its zero resistance makes it perfectly *diamagnetic*, make a superconducting enclosure an ideal magnetic shield. The diamagnetic property refers to its ability to exclude from its interior any externally applied magnetic field by the free flow of currents whose magnetic field exactly cancels throughout its interior the applied field.

Thus using known technology, there is great promise that systematic uncertainties in a  $Hg^+$  ion frequency standard can be pushed to levels inconceivable only a few years ago. Resonance frequency shifts due to the second-order Doppler effect, collisions, and magnetic field can be plausibly kept below parts in  $10^{16}$ ! Even the fractional frequency instability, which is a manifestation of the statistical error in fixing on the center of the resonance, can, by the use of multiple ion traps reach  $10^{-13} \tau^{-1/2}$ , where  $\tau$  is the averaging time. In the long term, for averaging times exceeding, say, one day, the *Allan variance*, the conventional measure of instability in frequency, would be less than  $4 \times 10^{-16}$ , surpassing all other standards.

## 17.4 The Proposed Ytterbium Ion Standard

The development of a *portable* laser-cooled  $Hg^+$  ion standard is handicapped by the difficulty in synthesizing its 194.2 nm ultraviolet resonance wavelength with an all solid-state laser optical system. In this regard there is a great deal of interest in the development of an ion standard based on another species, namely the ion of the mass 171 isotope of the rare earth element ytterbium ( $Yb^+$ ).

In Figure 17.4 the relevant energy levels for this isotope of  $Yb^+$  are shown, including (on a different scale) the 12.6 GHz magnetic hyperfine splitting of the ground state, which is used as the reference frequency, and the  $\lambda = 369.5$  nm ultraviolet transition used for hyperfine pumping and possible laser cooling. There are two essential differences between  $Yb^+$  as a reference ion and the  $Hg^+$  ion: First, the former has an ultraviolet resonance wavelength that is accessible by a simple

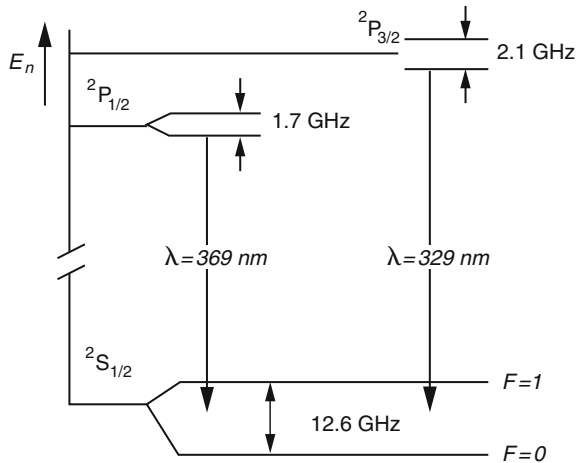


Figure 17.4 The relevant low-lying energy levels for a proposed  $\text{Yb}^+$  ion standard

doubling of the frequency of a diode laser output; second, the  $\text{Hg}^+$  ion reference frequency at 40.5 GHz is over three times larger than that for  $\text{Yb}^+$ , which under equal conditions makes the  $\text{Hg}^+$  ion resonance have a Q-factor three times greater and the standard based on it three times more stable. Nevertheless, until laser technology advances to the point where the synthesis of the ultraviolet frequency for the  $\text{Hg}^+$  ion becomes possible using small solid-state components, the  $\text{Yb}^+$  ion is a promising contender for field applications.

## 17.5 The Laser Pumped Cesium Beam Standard

### 17.5.1 The NITS-7

An important early application of lasers to atomic Cs standards is the optically pumped thermal beam standard; the one constructed at NITS, Boulder, and designated NITS-7 is a good example. Similar thermal Cs beam standards, substituting optical pumping for state-selecting magnets, have been put into operation in several standards laboratories around the world. They are very similar to the older magnetic deflection Cs standards, differing only in the method of state selection and the detection of clock transitions. In terms of both of these functions, laser pumping and detection have clear advantages over the classical methods. First, magnetic state selection removes from the beam those atoms that are in the wrong hyperfine state, whereas optical pumping simply transfers them from one to the other of the two clock states. Second, the fluorescence detection of the number of atoms that have made a clock transition is made nearly 100% efficient by using

a second laser to excite a strong second optical transition, chosen to be a *cycling transition*, that is, one allowed just between a given pair of levels. An atom that has made a clock transition can therefore repeatedly emit fluorescent photons differing in wavelength from those involved in hyperfine pumping, without leaving the two states. The third principal advantage relates to the absence of what might be called “chromatic aberration” in the magnetic state selection of atoms, that is, the dependence of the trajectories of the atoms on the distribution of their thermal velocities.

### 17.5.2 Laser diodes for Cs pumping

We recall that the Cs resonant fluorescence wavelength  $\lambda = 852$  nm is fortunately attainable directly using compact solid-state diode lasers; the type commonly used because of their spectral quality are called distributed Bragg reflection (DBR) diode lasers. These diode laser-based systems must, however, meet stringent requirements as to spectral purity and frequency stability in order to select particular optical hyperfine transitions. This requires active control of the laser output frequency, not with respect to an absolute reference optical cavity, as is often done, but with respect to a particular hyperfine component in the optical spectrum of cesium itself. This is done using a special absorption cell containing cesium vapor. However, unless special techniques are used, the spectral width of the resonance spectrum in such a cell would be too great for it to serve as a useful reference, due to the Doppler effect. In the days before the laser, efforts to reduce the Doppler width led to the development of atomic beams; now we have another approach, made practicable by the laser, called *saturated absorption* spectroscopy. It involves using two identical laser beams made to pass through the atomic vapor in opposite directions, in effect producing a *stationary* wave. If the laser beams cause a sufficiently high transition rate, there results a significant depletion in the number of those lower-state atoms whose Doppler-shifted frequency is resonant with the laser field, a depletion that indicates the beginning of saturation. If we imagine a third (weak) probing laser beam swept in frequency across the atomic resonance line, we would see successively absorption by different groups of atoms as their Doppler-shifted frequency comes into resonance with the probing beam, absorption that reflects the distribution of velocity among the atoms. However, two notches would appear in the absorption versus frequency curve, symmetrically placed about the maximum, as shown in Figure 17.5.

The frequency width of these notches, which following W. Bennett are referred to as “holes,” is the width the atoms would exhibit in the absence of the Doppler effect. This “hole burning” is due to the saturation of the absorption by those atoms whose Doppler-shifted frequency is resonant with one or the other of the two laser beams. By varying the frequency of these two beams, the two holes can be made to coalesce at the maximum of the Doppler curve, corresponding to selecting atoms that are resonant with both beams at the same time, that is, those that have near



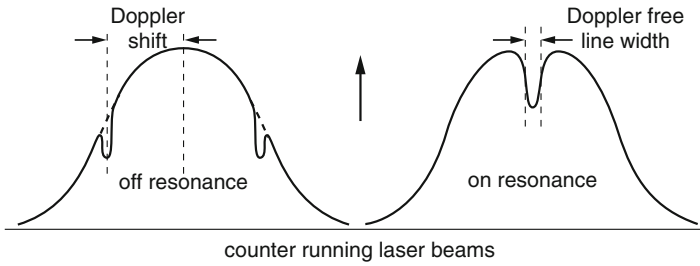


Figure 17.5 “Hole-burning” due to saturation in the Doppler broadened absorption profile

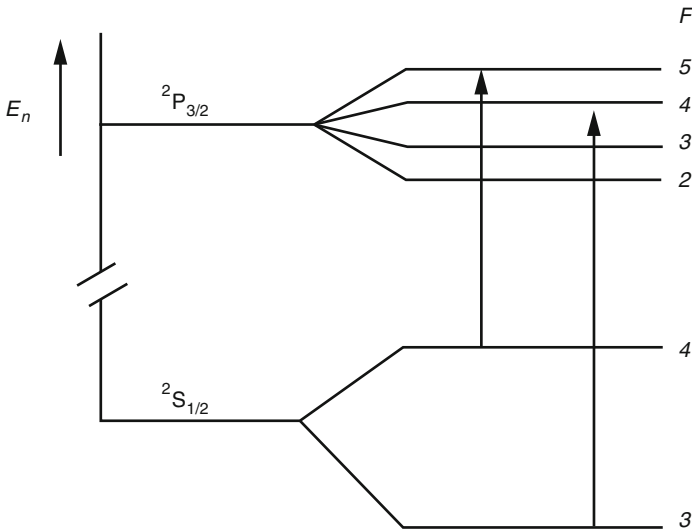


Figure 17.6 The transitions in Cs used to stabilize the diode lasers

zero velocity. This, then, is the basis of the *saturated absorption* technique for circumventing the Doppler broadening of spectral lines.

Using saturated absorption in a Cs vapor cell, the frequency of the output of one diode-based laser system ( $L_1$ ) is locked, by a servo-control loop, precisely on the frequency of the resonance  $D_2$  transition between the  $F = 4$  and  $F' = 5$  hyperfine states of the ground ( $^2S_{1/2}$ ) and first excited ( $^2P_{3/2}$ ) states respectively, as shown in Figure 17.6. The other laser ( $L_2$ ) is locked on the  $F = 4 \rightarrow F' = 3$  transition frequency, and induces transitions between those states, followed quickly by transitions to either  $F = 3$  or  $F = 4$  according to a certain branching ratio. The result after several photon absorptions is that the atoms end up mostly in the  $F = 3$  sublevel. This performs the function of the state-selecting A-magnet in the old standard. The other diode  $L_1$  induces the so-called cycling transition between

$F = 4$  and  $F' = 5$ , which is followed quickly by the emission of fluorescence radiation as the atom returns to the original sublevel  $F = 4$ . This is a cycling transition because the transition to  $F = 3$  is forbidden since electric dipole transitions must obey  $\Delta F = 0, \pm 1$ ; therefore any given atom in the  $F = 4$  sublevel can repeatedly absorb and reemit many fluorescent photons. That is the basis of the claim that as a detector of transitions into the  $F = 4$  sublevel it is 100% efficient. Clearly an essential requirement for this scheme to work is that the hyperfine spectrum is well resolved, both in terms of the spectral width of the two required lasers, and the fluorescence detection system.

The Ramsey cavity of NBS-7 is 1.55 m long; the line width of the central peak in the Ramsey pattern is 65 Hz corresponding to a  $Q \approx 1.5 \times 10^8$ . The cavity ends are carefully designed to minimize leakage of microwave power that would lead to Doppler-related phase shifts. The flow of microwave energy, as measured by the Poynting vector, should be zero at the center of the atomic beam window.

The microwave source for inducing the clock transition at 9.192 GHz is obtained by adding to the output of a low noise microwave multiplication chain at 9.18 GHz a low phase-noise, stable 10.7 MHz signal derived from a computer-controlled direct digital synthesizer (DDS) of fine resolution (see Chapter 4). The ultimate frequency reference is a hydrogen maser. The error signal needed to lock the frequency to the center of the atomic resonance is obtained using square frequency modulation at a rate of about 0.5 Hz.

### 17.5.3 Corrections to the Observed Cs Frequency

The principal types of corrections which must be applied to the observed resonance frequency in a beam standard have already been outlined in Chapter 9. As a standard, all possible sources of systematic error must be analyzed and evaluated to establish the accuracy with which it embodies the definition of the unit of time. Naturally the more ambitious the target accuracy is, the greater the number of subtle effects that become significant and must be evaluated. In the present case the *light shift* due to stray fluorescent light entering the Ramsey cavity would impose a grave limitation on the accuracy of this type of standard, if properly operated shutters are not provided to eliminate that possibility. Also the effects of spurious transients and sidebands in the interrogating microwave field, particularly accompanying the use of digital electronics must be brought within acceptable tolerance. This involves appropriately blanking the signal, with important consequences on the performance of the servo that locks the local oscillator to the atomic resonance.

If the various experimental parameters such as microwave power applied to the Ramsey cavity, the intensity of the magnetic field, the temperature of the Cs oven, etc. are automatically stabilized to their optimum values, the frequency synthesizer can be programmed to give the corrected output frequency, on any desired time scale. The essential performance figure for NBS-7, namely the uncertainty in its output frequency is reported to be about one part in  $2 \times 10^{14}$ , that is, about an order

of magnitude better than NBS-6, its magnetic predecessor. Ultimately they are both up against the available observation time set by the mean thermal velocity of around 100 m/s and the length of the standard.

## 17.6 The Cesium Fountain Standard

### 17.6.1 Using Gravity to Return Atoms

We will now take up the subject of what has become the most accurate reduction to practice of the definition of the unit of time as the duration of a certain number of oscillations in a Cs atom: the cesium fountain standard. In national standards laboratories around the world the cesium fountain is superseding the horizontal thermal beam standard.

The cesium fountain is a remarkable example of how the advent of laser cooling techniques made possible the practical realization of an early bold idea for increasing the precision of atomic/molecular beam resonance spectroscopy: the molecular *fountain* experiment, proposed by Zacharias in 1953 (Zacharias, 1954). In this, the limitation on the length, and hence resolution of a horizontal beam machine due to the curvature of the path under gravity would be removed by using a *vertical* beam in which the atoms follow narrow parabolic trajectories, reaching a height dependent on their initial velocity before falling back to the initial plane. Only one transition cavity would be required for a Ramsey pattern since the atoms could traverse the same cavity twice: going up and coming down. Since atoms starting with initial velocities higher than the limit set by the height of the apparatus are lost, only those at the slow end of the Maxwellian distribution would return to contribute to the resonance signal. For an apparatus of height  $h$  the maximum source velocity of returning particles is given by  $1/2MV^2 = Mgh$ , that is,  $V = (2gh)^{1/2}$ ; if for example  $h = 1.8$  m then  $V \approx 6$  m · sec<sup>-1</sup>, and the average time of flight of an atom about 1.2 sec. Unfortunately, for an atom such as Cs (mass number 133), this would be about the average velocity of particles in thermal equilibrium at a temperature of about 0.5° above absolute zero. At ordinary operating temperatures of an old Cs beam source, say 50°C, the number of atoms having a velocity below 6 m · sec<sup>-1</sup> would be so small, especially after some inevitable loss through scattering from background particles, that this approach would be not only impractical, but one in which the gain in spectral line narrowing would be offset by a loss in signal-to-noise ratio. Zacharias's attempt in fact failed.

But this is precisely the sort of problem that has been spectacularly overcome by the laser-cooling and capturing techniques we discussed in the last chapter. In fact, at the micro-kelvin range of temperatures attainable with laser cooling, a horizontal atomic beam cannot be formed at all with the usual geometry (except in microgravity, for example on the international space station); the parabolic arcs characteristic of bodies falling under gravity would have a strong downward trend that approaches a vertical descent.

One further critical requirement in order to fully achieve the potential of an atomic fountain standard is the “launching” of the atoms along a sufficiently narrow path as to form a fountain in which most of the atoms traversing the microwave field in the upward direction will return through it in the downward direction. The effusion of atoms from an orifice as in a conventional atomic beam source would be unacceptably slow and divergent. Ideally, the cooled atoms should be concentrated in a small space, put into the proper hyperfine state, and projected vertically upward along the axis. If a strong laser pulse, tuned to resonance, is used to provide the impulse, a small transverse velocity spread will inevitably be caused by the re-emitted fluorescent photons. An alternative method is to use a *moving optical molasses* to launch the atoms, that is, an optical molasses in which a frequency offset is introduced between the vertical pair of oppositely directed laser beams (both of which have their frequency offset below the atomic resonance); this, through the Doppler effect, is equivalent to referring the motion of the atoms to a moving frame of reference. The properties of the molasses are therefore the same in this moving frame of reference as they would be in the rest frame, in the absence of the frequency offset.

In 1989 appeared the first published account by a group at Stanford University of a successful experiment to produce a cold atomic fountain of another alkali element, sodium. The source was a magneto-optical trap (MOT) loaded from a thermal Na beam that was slowed by a counter-propagating frequency chirped laser beam. The atoms were cooled using a CW dye laser to generate the yellow resonance wavelength  $\lambda = 589.6$  nm of sodium corresponding to the ( $^2S_{1/2}, F = 2$ )  $\rightarrow$  ( $^2P_{3/2}, F' = 3$ ) transition. The relevant states in the sodium atom are shown in Figure 17.7. Actually the laser was tuned 20 MHz below the exact resonance in accordance with the laser cooling technique, and a sideband frequency resonant with the  $F = 1 \rightarrow F' = 2$  transition was generated by an electro-optic modulator (EOM) in order to counteract the pumping of states out of the  $F = 2$  sublevel. This is rendered necessary by the fact that evidently the laser spectral line width did not completely resolve the smaller hyperfine intervals in the  $2P_{3/2}$  state. The modulator is turned off when the atoms must be pumped into the lower  $F = 1$  state for the purposes of observing the microwave resonance.

The atoms were ultimately cooled to a temperature of 50  $\mu\text{K}$ , at which point the spherical atomic distribution, “the ball” that is “tossed”, has a radius of 2 mm. A pulsed laser beam imparts to it a vertical velocity of about 240  $\text{cm s}^{-1}$ ; recoil from the fluorescent photons contributes to a transverse spread in velocity of 22  $\text{cm s}^{-1}$ . The transition cavity is a section of waveguide placed near the top of the atoms’ ballistic trajectory. A bias uniform magnetic field of intensity around  $2 \times 10^{-6}\text{T}$  was applied to separate the field-dependent transitions. The interrogation field is applied in two successive  $\pi/2$  pulses separated by an interval 255 ms, giving a central Ramsey peak with a full width at half maximum (FWHM) of 2.0 Hz.

This demonstration of the remarkably narrow resonance obtainable with an atomic fountain was followed by its first application to a primary frequency

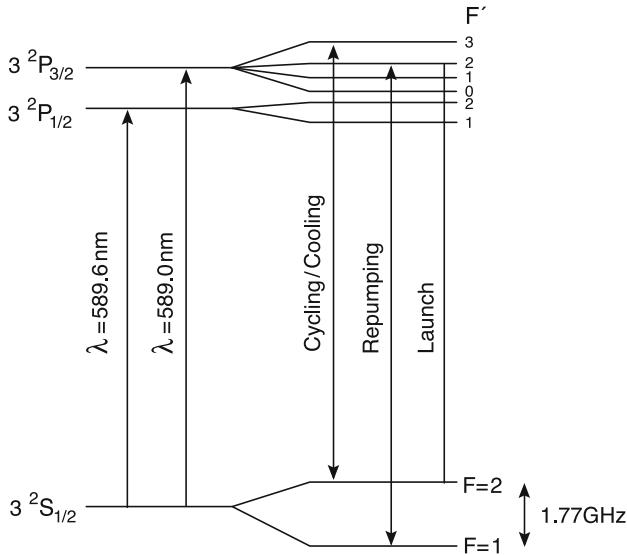


Figure 17.7 The relevant quantum energy levels in sodium

standard around 1994 by the group at the Laboratoire Primaire du Temps et Fréquence (BNM-LPTF) Paris. An account of the first NIST Boulder Cs fountain NIST-F1 was published in 1999. Several national standards laboratories including the National Physical laboratory (NPL), Physikalisch-Technische Bundesanstalt (PTB) and Istituto Elettrotecnico Nazionale (IEN) have now operational Cs fountain standards with an accuracy around  $10^{-15}$ . If a standard could maintain this stability for 31.7 million years, it would lose or gain one second!

### 17.6.2 The Prototype at the Paris Observatory

As an interesting introduction to the design and operation of a cold Cs fountain standard we will describe the historically significant first prototype Cs fountain standard at the LPTF of the Paris Observatory (Santarelli, 1994). Figure 17.8 shows schematically the essential elements of such a standard. There are four principal functions that must be performed on the atoms: First, they must be cooled and accumulated in a source and projected up; second, they must be put preferentially in the lower of the two hyperfine substates of the ground state; third, they must freely follow their vertical trajectories in a weak uniform magnetic field (the C-field), interacting with the clock frequency microwave field only at the beginning and end of their journey (the Ramsey field); and finally, their hyperfine sublevel population must be monitored to detect clock transitions. The first two functions are fulfilled in the laser-cooled source, while the Ramsey method of inducing transitions takes the form here of phase-coherent excitation experienced sequentially

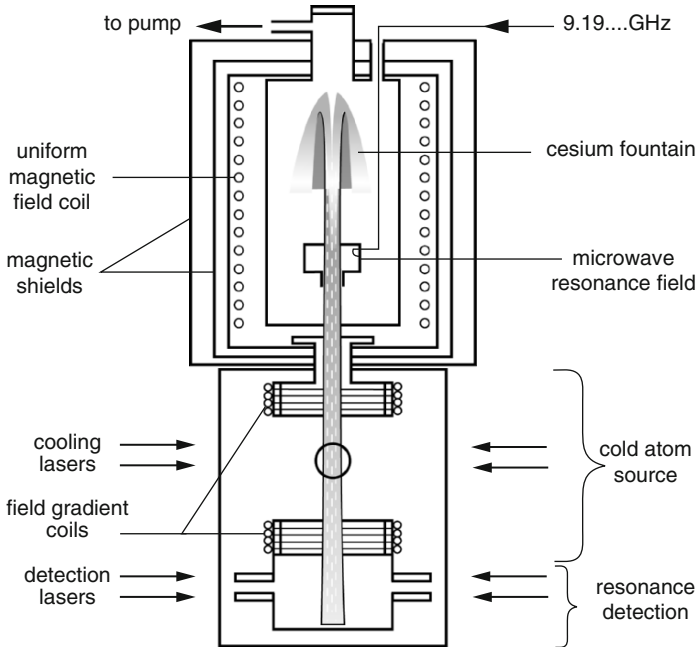


Figure 17.8 A schematic sketch of the Paris Observatory prototype cesium fountain standard (Santarelli, 1994)

in time as the atoms pass through the same cavity going up and then coming down, rather than the space-separated regions in a classical Ramsey cavity. Finally, the measurement of the transition probability is achieved optically using the detection of resonance fluorescence from a cycling transition which the narrow spectral width of the laser light permits to be excited selectively. The Paris Observatory prototype was reported to have a cold atom source in which as many as  $10^8$  atoms are trapped and could be cooled to as low as 5 micro-degrees above absolute zero. It uses the now familiar three pairs of mutually perpendicular laser beams tuned below the resonance maximum, and can be operated as a pure  $lin \perp lin$  optical molasses or as a magneto-optical trap (MOT) with a magnetic field gradient ( $-8 \times 10^{-2}$  T/m) produced by two current-opposed Helmholtz coils. The cold atoms are projected up through the Ramsey microwave cavity ( $Q = 30,000$ ) and into the 70 cm long Ramsey ballistic path region, 30 cm above the cold source, using the moving molasses technique. A highly uniform and constant magnetic field ( $B = 1.7 \times 10^{-7}$  T) is provided in the Ramsey region by a coaxial solenoid with correction end coils inside four layers of magnetic shielding from outside disturbances. The background gas pressure is kept under  $10^{-8}$  Pa to minimize the loss of projected atoms by scattering off residual gas particles. The overall length of the standard is about 1.5 m.

The optical system is built around four diode lasers with sharp spectral output: one external cavity diode laser is stabilized using saturated absorption in a Cs cell and tuned 2 MHz below the cycling transition  $F = 4 \rightarrow F' = 5$  used for both cooling and detection of clock transitions. This laser is used to injection-lock through an acousto-optic modulator (AOM) two high power 100 mW diodes that are used in the formation of the pairs of beams needed to create the atomic molasses in the source. A fourth “repumper” diode laser is required, tuned to the  $F = 3 \rightarrow F' = 4$  transition, to offset the pumping of atoms out of the  $F = 4$  level by the cooling lasers. The laser beams are spatially filtered and expanded to 1.5 cm diameter with a maximum power around  $10 \text{ m W/cm}^2$  for cooling and  $1 \text{ m W/cm}^2$  for detection.

The fountain standard is operated sequentially through several stages. First the magneto-optical trap (or optical molasses) must be loaded with atoms; the lasers at this stage are set at their maximum power and detuned below resonance by  $3\Gamma$ , where  $\Gamma$  is the natural optical linewidth of Cs. This phase is completed in about 0.4 s, the atoms reaching a temperature of about  $60 \mu\text{K}$ . The next stage is the launching of the atoms, accomplished most satisfactorily using the moving molasses technique, which we recall entailed raising the frequency of the upward vertical beam relative to the downward one. An upward velocity of 5 m/s was achieved in 0.2 ms. The process heats up the atoms and the molasses lasers are again turned on at full intensity with the  $3\Gamma$  detuning. Finally the cooling is extended using weaker intensities and  $10 \Gamma$  detuning of the lasers to reach, it is reported, an ultimate temperature of about  $5 \mu\text{K}$ .

In the next phase the atomic cloud enters the microwave cavity driven in the  $\text{TE}_{011}$  mode to induce the first  $\pi/2$  of the clock transition at 9.192 GHz. For a standard, the source of the interrogating microwave field must have very low noise and high spectral purity, free of spurious transients. The method of synthesizing that frequency in the prototype exploits the low noise short term stability of a dielectric resonator oscillator (DRO), which is phase locked to a stable frequency synthesized from a high harmonic of a 10 MHz quartz oscillator (referenced to an H-maser) and a lower frequency synthesizer. This synthesizer is programmed to set the frequency alternately on the two sides of the central fringe of the Ramsey pattern.

The final phase is the detection of the number of atoms that have made the clock transition as a fraction of the total number, and the measurement of the vertical velocity distribution of the atoms as they fall through the detection region. First, the atoms are subject to a pair of counter-propagating beams detuned 2 MHz below the  $F = 4 \rightarrow F' = 5$  transition frequency; the resulting fluorescence is detected as a measure of the number of atoms that have made the clock transition. This is followed by subjecting the atoms to just one traveling wave beam causing atoms in the  $F = 4$  level to be pushed aside and the atoms in the lower  $F = 3$  level, that have not made a clock transition are then pumped into the  $F = 4$  level and their number measured by their fluorescence as before.

The striking features of the Ramsey pattern obtained with this fountain standard is the large number of resolved fringes indicating fairly monoenergetic atoms and the relatively narrow Rabi envelope due to the relatively long cavity. The central

Ramsey fringes obtained are reported to be 700 mHz obtained with a 500 ms flight time. Using the two-sample Allan variance formula:

$$\sigma_y(2, \tau) = \frac{\Delta\nu}{\pi\nu_0} \left(\frac{N}{S}\right) \sqrt{\frac{T_C}{\tau}} \quad 17.8$$

where  $\Delta\nu$  is the line width,  $S/N$  the signal to noise ratio for one cycle and  $T_C$  the period of one cycle. Substituting the experimental value  $S/N \approx 300$  we find  $\sigma_y = 10^{-13}\tau^{-1/2}$ , or  $3 \times 10^{-15}$  over a period of 1000 seconds. This is two orders of magnitude improvement over the classical thermal beam standards.

Finally, we note that an atomic fountain standard not only has a sharper resonance and therefore enhanced frequency stability, but can also reduce some important sources of systematic error. Errors arising from asymmetry in the microwave resonance field are reduced by the passage of the fountain in both directions through the same field, as is the (second-order) Doppler shift because of the low velocity of the atoms. These advantages clearly justify its adoption as a fixed installation primary standard of the highest accuracy.